Article ID: 1006-8775(2018) 02-0220-12

THE DOUBLE–LAYER STRUCTURE OF THE HADLEY CIRCULATION AND ITS INTERDECADAL EVOLUTION CHARACTERISTICS

CHENG Jian-bo (成剑波), HU Shu-juan (胡淑娟), CHOU Ji-fan (丑纪范)
(College of Atmospheric Sciences, Lanzhou University, Lanzhou 73000 China)

Abstract: Based on the three-pattern decomposition of global atmospheric circulation (TPDGAC), this study investigates the double-layer structure of the Hadley circulation (HC) and its interdecadal evolution characteristics by using monthly horizontal wind field from NCEP/NCAR reanalysis data from 1948—2011. The following major conclusions are drawn: First, the double-layer structure of the HC is an objective fact, and it constantly exists in April, May, June, October and November in the Southern Hemisphere. Second, the double-layer structure is more obvious in the Southern than in the Northern Hemisphere. Since the double-layer structure is sloped in the vertical direction, it should be taken into consideration when analyzing the variations of the strength and location of the center of the HC. Third, the strength of the double-layer structure of the HC in the Southern Hemisphere consistently exhibits decadal variations with a strong, weak and strong pattern in all five months (April, May, June, October, and November), with cycles of 20–30 a and 40–60 a. Fourth, the center of the HC (mean position of the double-layer structure) in the Southern Hemisphere consistently and remarkably shifts southward in all the five months. The net poleward shifts over the 64 years are 5.18°, 2.11°, 2.50°, 1.79° and 5.76° for the five respective months, with a mean shift of 3.47°.

Key words: three-pattern decomposition of global atmospheric circulation; Hadley circulation; double-layer structure; decadal variations

CLC number: P467 **Document code:** A

doi: 10.16555/j.1006-8775.2018.02.010

1 INTRODUCTION

The Hadley circulation (HC), one of the most prominent global atmospheric circulation patterns, has a rising motion near the equator and a sinking motion in the subtropics, corresponding to the intertropical convergence zone and the subtropical high, respectively. The HC has significant impacts on the global climate system by transporting heat, water vapor and angular momentum between the tropics and the extratropics [1–2]. Because of the critical weather and climate implications of the HC, there has been a substantial interest in changes in the HC in recent decades, focusing mainly on its intensity and meridional width.

Many studies have suggested a strengthening trend of the HC in recent decades, especially for the boreal winter HC [3–9]. For example, Wielicki et al.[3] and Chen et al. [4] reported an increase in outgoing longwave radiation (OLR) in the subtropics, suggesting a strengthening of tropical circulations, particularly the HC. In previous studies, the intensity of the HC was generally defined as the maximum (minimum) value of the mean meridional mass stream-function (MMS). However, based on the MMS from 1979 to 1984 calculated using an iteration scheme[10], the double-layer structure of the HC derived from ERA-15 reanalysis was identified [11]. In addition, by investigating the HC from 1979 to 1989, Yue et al.[12] and Qing et al.[13] also suggested that there exists a double-layer structure in the HC, and this double-layer structure is sloped in the vertical direction. These studies raise the following issue: The intensity of the HC, which contains a double-layer structure, should be defined as the average of the maximum (minimum) values of the two centers. However, in many previous studies, the double-layer structure of the HC is not taken into consideration, and the maximum (minimum) value of the MMS in the tropics is commonly used to represent the intensity of the HC, leading to bias in the analysis. Thus, the study of the double-layer structure is vital for the accurate description of the intensity and location of the HC.

On the other hand, a poleward expansion of the HC over the past few decades has been found in recent studies. Since the descending branch of the HC is closely related to the subtropical semi-arid area, the poleward expansion of the HC, which may lead to less precipitation and enhanced drought in the subtropics, has fundamental impacts on the global climate, especially the subtropical climate. By using three reanalyses and three OLR datasets, Hu and Fu [14]

Received 2017-08-22; **Revised** 2018-02-28; **Accepted** 2018-05-15

Foundation item: National Natural Science Foundation of China (41475068, 40805034); Special Scientific Research Project for Public Interest (GYHY201206009); Fundamental Research Funds for the Central Universities of China (lzujbky-2014-203)

Biography: CHENG Jian-bo, Ph.D. candidate, primarily undertaking research on climate dynamics.

Corresponding author: HU Shu-juan, e-mail: hushuju@lzu.edu.cn

suggested a robust poleward expansion of the HC since 1979, with the most prominent expansion in summer and autumn of both hemispheres. The poleward shift of the HC can also be determined by many other indicators [15-18], such as the tropopause height, total column ozone, precipitation, and position of subtropical jet, among others. The observed expansion of the HC can be reproduced by climate models but with a much smaller magnitude compared to that derived from various reanalyses and observations [19-20]. Since changes in the meridional extent of the HC vary differently between reanalyses and climate models and among different indicators, new methods and data are needed to confirm the expansion.

Recently, Xu [21], Hu et al. [22-26] and Liu et al. [27] proposed a new method termed the three-pattern decomposition of global atmospheric circulation (TPDGAC). Based on the essential features of global atmospheric circulation, the three-dimensional (3D) horizontal, meridional and zonal circulations, which can be considered as the global generalization of the Rossby wave in the middle and high latitudes and the Hadley and Walker circulations in the low latitudes, have been defined to decompose the global atmospheric circulation into a superposition of the three large-scale circulations. By combining atmospheric circulations in the low and middle-high latitudes, the TPDGAC provides a complete description of global large-scale atmospheric circulations. The TPDGAC may also be helpful to uncover the mechanisms of the complicated interactions between the atmospheric circulations at middle and high latitudes and low latitudes and those among the horizontal, meridional and zonal circulations.

The remainder of this paper is organized as follows. A brief introduction of the TPDGAC is presented in Section 2. A new data set of the three-pattern circulations (horizontal, meridional and zonal circulations) can then be obtained by interpolating the NCEP/NCAR reanalysis data into the TPDGAC. By using the new data, the double-layer structure of the HC is studied in Section 3, and the changes in the intensity and location of the center of the HC are investigated in Section 4. Finally, a summary is given in Section 5.

2 DATA AND METHODS

2.1 *Data*

The data used in this study are the monthly mean zonal wind and meridional wind from NCEP/NCAR reanalysis data with a 2.5°×2.5° horizontal resolution. In the vertical direction, the commonly used 17 pressure levels are used. The analyzed time period in this study is from 1948 to 2011.

2.2 *Analysis methods*

The analysis methods used in this study are the TPDGAC, Gaussian low-pass filter, wavelet analysis method and Mann-Kendall method.

2.3 *Three-pattern decomposition of global atmospheric circulation*

For convenience, we briefly introduce the TPDGAC and related symbols in this section. To solve the unit inconsistency in the calculation of the 3D vorticity vector in the p-coordinate system, the spherical σ-coordinate system is introduced in the TPDGAC, namely,

$$u'=\frac{u}{a},\ v'=\frac{v}{a},\ \dot{\sigma}=\frac{\omega}{p_s},\ \sigma=\frac{p-p_0}{p_s-p_0},$$

where a is the earth's radius, p is the pressure, p_s=1,000 hPa is the pressure at the earth's surface, p_0=0 Pa is the pressure at top of the atmosphere. Here, $(u',\ v',\dot{\sigma})$ and $(u,\ v,\ \omega)$ represent the three velocity components in the spherical σ-coordinate system and spherical p-coordinate system, respectively.

The global 3D horizontal circulation $\vec{V}'_R$, meridional circulation $\vec{V}'_H$ and zonal circulation $\vec{V}'_W$ are defined as follows:

$$\vec{V}'_R=\vec{i}u'_R(\lambda,\theta,\sigma)+\vec{j}v'_R(\lambda,\theta,\sigma),$$

$$\vec{V}'_H=\vec{j}v'_H(\lambda,\theta,\sigma)+\vec{k}\dot{\sigma}_H(\lambda,\theta,\sigma),$$

$$\vec{V}'_W=\vec{i}u'_W(\lambda,\theta,\sigma)+\vec{k}\dot{\sigma}_W(\lambda,\theta,\sigma),$$

and the following continuity equations are satisfied:

$$\begin{cases} u'=u'_W+u'_R=\dfrac{\partial W}{\partial\sigma}-\dfrac{\partial R}{\partial\theta}, \\ v'=v'_R+v'_H=\dfrac{1}{\sin\theta}\dfrac{\partial R}{\partial\lambda}-\dfrac{\partial H}{\partial\sigma}, \\ \dot{\sigma}=\dot{\sigma}_H+\dot{\sigma}_W=\dfrac{1}{\sin\theta}\dfrac{\partial(\sin\theta H)}{\partial\theta}-\dfrac{1}{\sin\theta}\dfrac{\partial W}{\partial\lambda}, \end{cases} \qquad (1)$$

where H, W and R are the stream functions of the meridional, zonal and horizontal circulations, respectively.

According to Eq. (1), if the stream functions H, W and R are given, the velocity components of the three-pattern circulations $\vec{V}'_H$, $\vec{V}'_W$ and $\vec{V}'_R$ and the 3D velocity field of the actual atmospheric circulation can be obtained. On the contrary, the stream functions H, W and R can be calculated by using the velocity field of the actual atmospheric circulation. Thus, the global atmospheric circulation is decomposed into a superposition of the horizontal, meridional and zonal circulations.

It is evident that Eq. (1) cannot guarantee the uniqueness of the stream functions H, W and R because the three-pattern circulations $\vec{V}'_H$, $\vec{V}'_W$ and $\vec{V}'_R$ have three spatial dimensions. To guarantee the mathematical uniqueness and physical rationality of the TPDGAC, the stream functions H, W and R should satisfy the following restrictive condition:

$$\frac{1}{\sin\theta}\frac{\partial H}{\partial\lambda}+\frac{1}{\sin\theta}\frac{\partial(W\sin\theta)}{\partial\theta}+\frac{\partial R}{\partial\sigma}=0 \qquad (2)$$

with the following boundary conditions:

when σ=1, we have

$$H=W=0 \text{ and } \frac{\partial R}{\partial \sigma}=0 \tag{3}$$

By plugging Eqs. (2) and (3) into Eq. (1), the following three boundary value problems of the stream functions H, W and R can be obtained:

$$\begin{cases} \Delta R=\frac{1}{\sin\theta}\frac{\partial v'}{\partial \lambda}-\frac{1}{\sin\theta}\frac{\partial(u'\sin\theta)}{\partial\theta}, (\lambda,\theta,\sigma)\in\Omega, \\ \frac{\partial R}{\partial n}\Big|_{\partial\Omega}=\frac{\partial R}{\partial\sigma}\Big|_{\sigma=1}=0, \end{cases} \tag{4}$$

$$\begin{cases} \frac{\partial H}{\partial \sigma}=\frac{1}{\sin\theta}\frac{\partial R}{\partial\lambda}-v', \quad (\lambda,\theta,\sigma)\in\Omega, \\ H|_{\partial\Omega}=H|_{\sigma=1}=0, \end{cases} \tag{5}$$

$$\begin{cases} \frac{\partial W}{\partial \sigma}=\frac{\partial R}{\partial\theta}+u', \quad (\lambda,\theta,\sigma)\in\Omega, \\ W|_{\partial\Omega}=W|_{\sigma=1}=0, \end{cases} \tag{6}$$

where $\Omega=S^2\times[0, 1]$, and $S^2=\{(\lambda,\theta)\,|\,0\leqslant\lambda\leqslant 2\pi, 0\leqslant\theta\leqslant 2\pi\}$ is a unit sphere surface. $\partial\Omega$ is the boundary of Ω and is also a unit sphere surface. n is the unit outer normal vector of $\partial\Omega$, and $\Delta=\frac{1}{\sin^2\theta}\frac{\partial^2}{\partial\lambda^2}+\frac{1}{\sin\theta}\frac{\partial}{\partial\theta}(\sin\theta\frac{\partial}{\partial\theta})+\frac{\partial^2}{\partial\sigma^2}$ is the 3D Laplacian in the spherical σ-coordinate system. Eqs. (1) and (2) represent the three-pattern decomposition model (TPDM), and the problems (4)–(6) are the definite solution problems of the TPDM.

It is evident that the solution to the boundary problems (4)–(6) is unique. Thus, if we plug the horizontal components of the velocity field $\vec{V}'$ into the boundary problems (4)–(6), the stream functions H, W and R can be obtained. Furthermore, the global atmospheric circulation can be decomposed into the three-pattern circulations $\vec{V}'_H$, $\vec{V}'_W$ and $\vec{V}'_R$ by using Eq.(1). The stream function of the meridional circulation H derived from Eqs. (1), (4), (5) and (6) is used for the following investigation. It should be noted that, different from traditional decomposition methods [11–13], the TPDGAC can decompose the vertical velocity into two parts, corresponding to the respective Hadley and Walker circulations. Effective decomposition of the vertical circulation into the Hadley and Walker circulations is convenient for the study of tropical overturning circulations.

3 DIAGNOSIS OF THE DOUBLE-LAYER STRUCTURE OF THE HC

3.1 *The double-layer structure from* $[\overline{v_H}]$

To maintain consistency with previous studies[10, 12, 13], we use the meridional wind $\overline{v_H}$ and stream function H of the meridional circulation from 1979 to 1989 for further investigation in Section 3.1 and Section 3.2, respectively. Wu and Liu [11] noted that the vertical profile of can be used as the criterion of the existence of the double-layer structure. '[ ]' represents the global zonal average, and '—' represents the time average. From the earth's surface to the top of the atmosphere, if the sign of $[\overline{v_H}]$ at a certain latitude changes three times, then we consider that there exists a double-layer structure in the HC at that latitude.

Figure 1 displays the climatology of the monthly mean zonally averaged (0–360°) meridional wind of the meridional circulation. It can be observed from Fig.1 that the sign of $[\overline{v_H}]$ changes three times for the Northern Hemisphere HC in April and October and for the Southern Hemisphere HC in January, July and October, implying that there exists a double-layer structure in these HCs.

It should be noted that Fig.1 in this study and Fig.3 in Yue et al.[12] are almost the same, namely, $[\overline{v_H}]=[\overline{v}]$ (v_H is the meridional wind of the meridional circulation, and v is the meridional wind from NCEP/NCAR reanalysis data). According to Eq.(14) in Liu et al.[27], we have $[\overline{v_H}]=[\overline{v}]-[\overline{v_R}]=[\overline{v}]$ and $[\overline{v_R}]=0$. In the actual calculation, we also find $[v_R]=0$, suggesting that the horizontal Rossby wave has been filtered and only the meridional wind of the HC is reserved when averaged globally. However, when averaged locally, we have $[v_R]\neq 0$ and $[v_H]\neq[v]$. When investigating the local HC, if we use $[v]$ to calculate the traditional MMS, there will be some errors since $[v]$ includes the information of the horizontal Rossby circulation. On the other hand, different from the globally averaged MMS, the meridional stream function H has three spatial dimensions. Thus, it may be more accurate to use the TPDGAC when investigating the local HC. Further examination of the local HC is beyond the scope of the present study and will be undertaken in future studies.

3.2 *The double-layer structure from* $[\overline{H}]$

Figure 2 displays the climatology (1979—1989) of the monthly mean zonally averaged (0–360°) meridional stream function $[\overline{H}]$. It can be observed from Fig.2 that the strength and location of the rising branch of the HC depend largely on the seasons. The rising branch of the HC shifts southward in January and northward in July. In either hemisphere, it is evident that the winter HC, with its rising motion in the tropics of the warm hemisphere and sinking motion in the subtropics at approximately 30° of the cold hemisphere, is stronger than the summer HC. In transition seasons, the Hadley circulations in both hemispheres are similar except for small differences in the intensity.

It is evident from Fig.2 that there are two centers in the Southern Hemisphere HC in April, suggesting two minimal values in the vertical profile of the meridional stream function $[H]$ at the latitude of the center of the HC. This implies that the Southern Hemisphere HC in April includes a double-layer structure. From the earth's surface to the top of the atmosphere, if there are two maximal (minimal) values of $[H]$, then we consider that there exists a double-layer

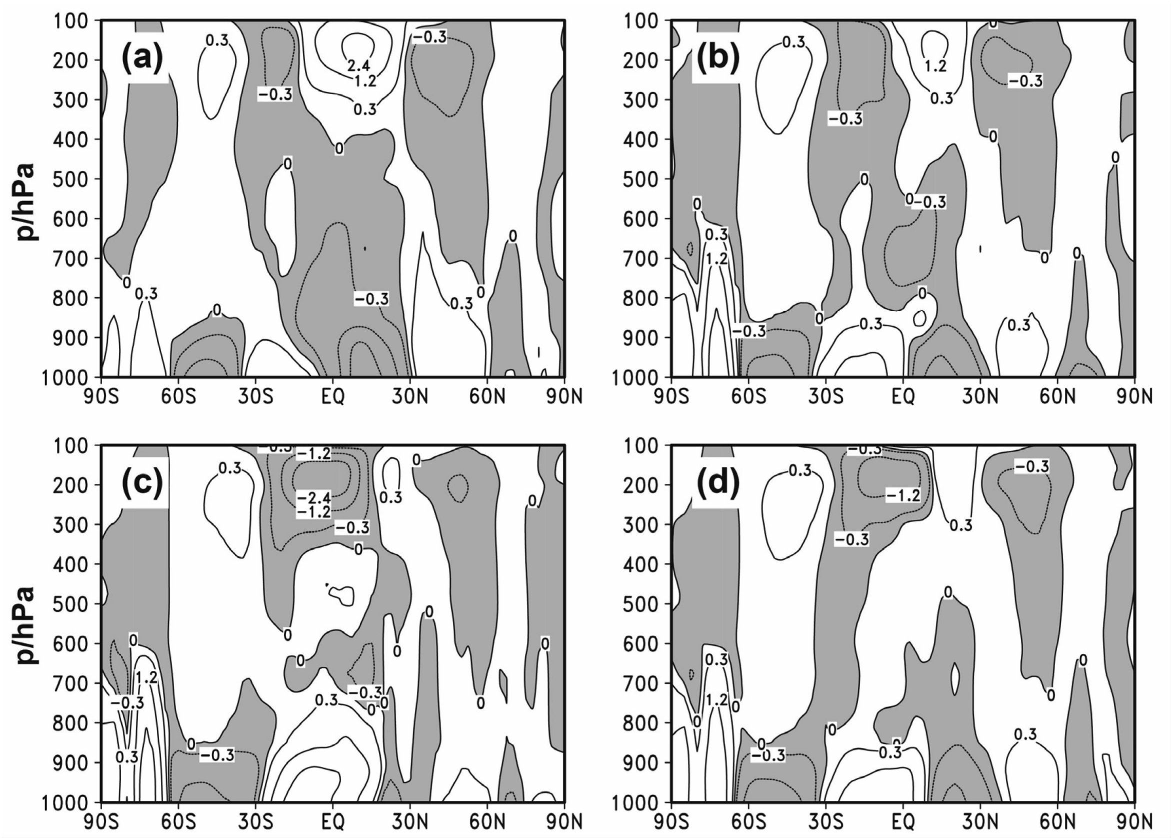

Figure 1. Mean state (1979–1989) of the zonally averaged meridional wind (m s^{-1}) of meridional circulation over the globe in (a) January, (b) April, (c) July and (d) October.

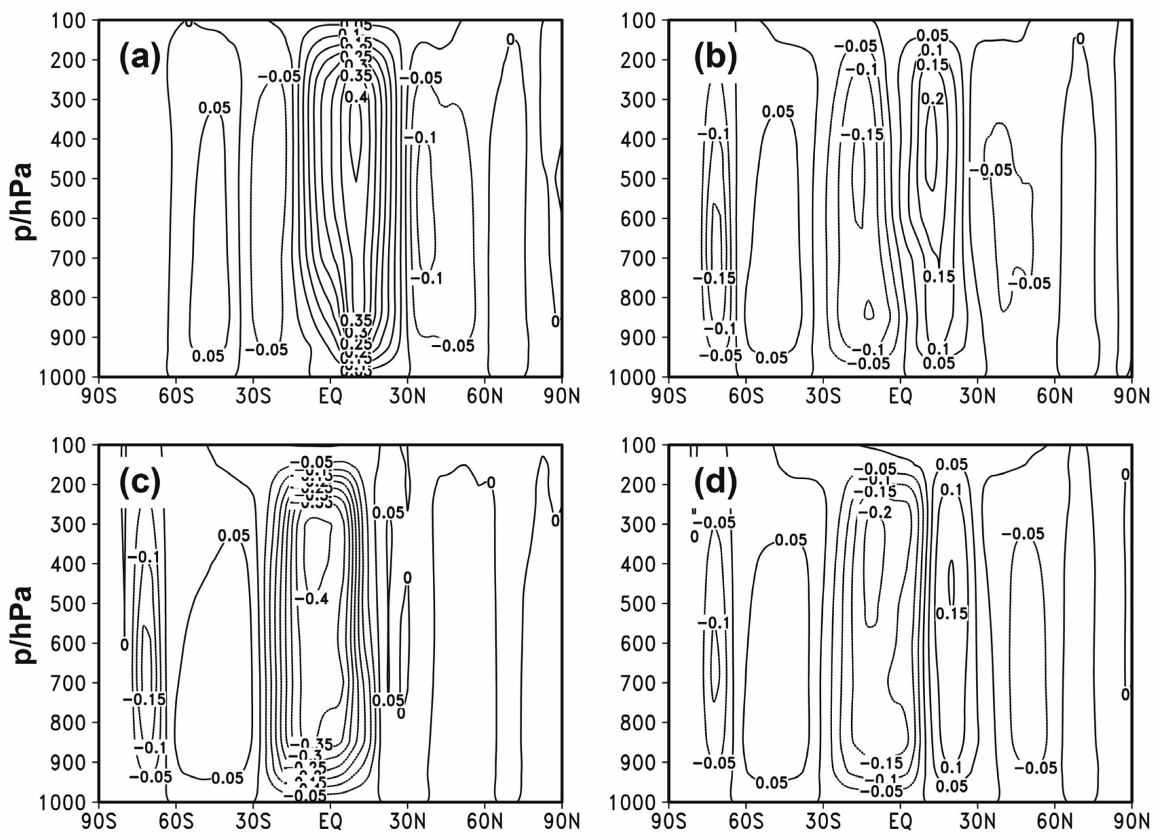

Figure 2. Mean state (1979–1989) of the zonally averaged stream function (10^{-6} s^{-1}) of meridional circulation over the globe in (a) January, (b) April, (c) July and (d) October.

structure in the HC at that latitude. Thus, the vertical profile of the meridional stream function $[\overline{H}]$ can also be used as the criterion of the existence of the double-layer structure[12]. First, we calculate the location of the center of the HC for both hemispheres in January, April, July and October year by year from 1979 to 1989. Second, we calculate the 11-year mean location of the center of these HCs. Third, according to the vertical profile of $[\overline{H}]$, we can make a judgment whether there exists a double-layer structure in these HCs.

The vertical distribution of the meridional stream function at the location of the centers of these HCs is shown in Table 1. It can be observed from Table 1 that the double-layer structure exists only in the Northern Hemisphere HC in July and the Southern Hemisphere HC in October. The double-layer structure in the Northern Hemisphere HC in July is quite weak since the maximal value of the upper center differs by 0.001×10^{-6} s^{-1} from the lower center. The results based on the meridional stream function $[\overline{H}]$ are quite different from those based on the meridional wind $[\overline{v_H}]$. The causes of the differences between the two criteria will be studied in Section 3.3 by investigating the detailed characteristics of the HC.

3.3 *Objective existence of the double-layer structure*

The two criteria of the double-layer structure of the HC proposed in Sections 3.1 and 3.2 are indirect methods, and the results based on these criteria differ. A natural question arises: Can we estimate the real double-layer structure by using the two criteria? To answer this question, we should investigate the detailed structure of the HC. To maintain consistency with the previous investigation in Sections 3.1 and 3.2, Fig.3 shows the detailed structure of the HC with an area S=725 ×15 (hPa·latitude) for both hemispheres in January, April, July and October from 1979—1989.

Figure 3 shows that the double-layer structure exists only in the Southern Hemisphere HC in April and October. The double-layer structure of the HC in the Southern Hemisphere in October can be observed using both criteria. However, the double-layer structure of the

Table 1. Vertical distribution of the meridional stream function (10^{-6} s^{-1}) at the location of the centers of HCs.

p/hPa	Jan	Apr		Jul		Oct	
	10.0°S	15.0°S	12.5°N	7.5°S	22.5°N	10.0°S	20.0°N
100	0.028	−0.004	0.014	0.004	0.031	0.008	0.016
150	0.128	−0.035	0.062	−0.059	0.042	−0.031	0.051
200	0.275	−0.086	0.140	−0.233	**0.053**	−0.130	0.094
250	0.371	−0.116	0.185	−0.366	0.051	−0.191	0.121
300	0.405	−0.133	0.201	−0.415	0.051	−0.214	0.137
400	**0.414**	−0.152	**0.213**	**−0.418**	**0.054**	**−0.216**	0.151
500	0.401	**−0.156**	0.209	−0.397	**0.054**	−0.207	**0.152**
600	0.383	−0.151	0.180	−0.386	0.047	−0.194	0.145
700	0.367	−0.147	0.143	−0.383	0.033	−0.174	0.141
850	0.362	−0.147	0.136	−0.359	0.016	**−0.184**	0.135
925	0.234	−0.105	0.104	−0.225	0.005	−0.134	0.093

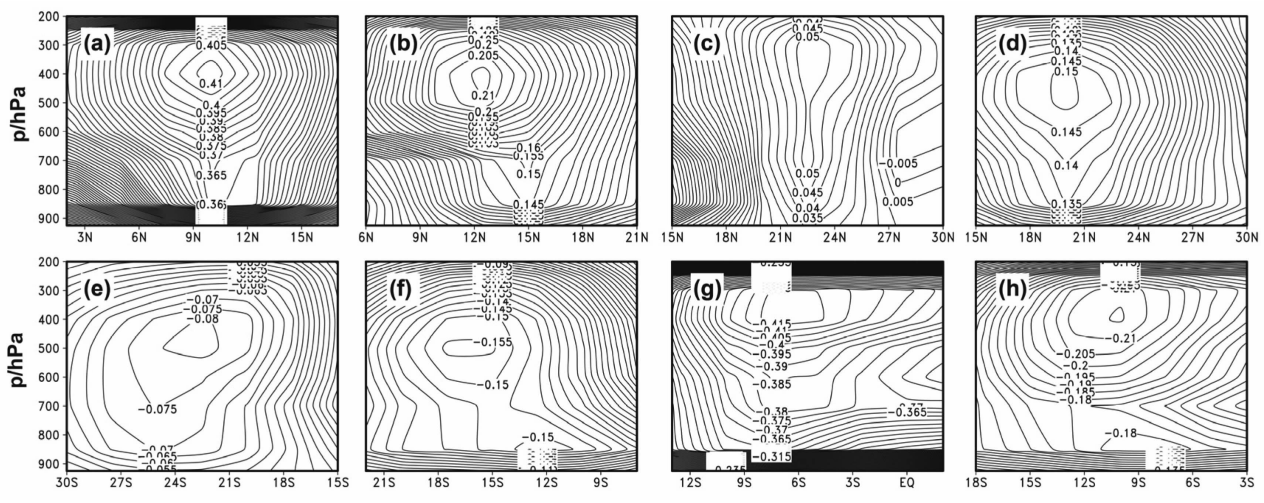

Figure 3. Detailed structure of the mean state (1979–1989) of the zonally averaged stream function (10^{-6} s^{-1}) of meridional circulation over the globe in (a) January, (b) April, (c) July and (d) October for the Northern Hemisphere and (e) January, (f) April, (g) July and (h) October for the Southern Hemisphere.

HC in the Southern Hemisphere in April cannot be observed using the criteria based on the vertical profiles of $[\overline{v_H}]$ and $[\overline{H}]$. This is because these criteria should limit the vertical profiles at a certain latitude, and the double-layer structure of the HC in the Southern Hemisphere in April is sloped in the vertical direction; consequently, the double-layer structure cannot be observed. The results based on the vertical profiles of $[\overline{v_H}]$ and $[\overline{H}]$ may be incorrect since the double-layer structure of the HC in the Northern Hemisphere in April and October and in the Southern Hemisphere in January and July cannot be observed in Fig.3. Thus, the detailed structure of the HC is vital to accurately estimate the double-layer structure.

The analysis proposed above is limited in January, April, July and October. By investigating the detailed structure of the HC in other months (data not shown), we find that the double-layer structure also exists in the Northern Hemisphere HC in August, September and December and in the Southern Hemisphere in May, June and November, implying the objective existence of the double-layer structure.

3.4 *Long–term existence of the double–layer structure*

We should confirm the long-term existence of the double-layer structure of the HC in this section since the time period of the analysis proposed is limited to the period from 1979 to 1989. Six 10-year periods, namely, 1951—1960, 1961—1970, 1971—1980, 1981—1990, 1991—2000, 2001—2010, are chosen to confirm the long-term existence of the double-layer structure of the HC. Table 2 displays the decadal evolution of the double-layer structure of the HC. In Table 2, HCs that include the double-layer structure are represented as 2; HCs that include the dumbbell-shaped structure are represented as 1; HCs that do not include the double-layer structure or the dumbbell-shaped structure are represented as 0. It can be observed from Table 2 that the number 2 appears four times and the number 1 appears twice for the Southern Hemisphere HC in April, May, June, October and November, suggesting a double-layer structure of these HCs. The long-term existence of the double-layer structure is confirmed, and the double-layer structure of the HC in the Southern Hemisphere is more obvious than that in the Northern Hemisphere.

4 DECADAL EVOLUTION CHARACTERISTICS OF THE HC

In this section, the evolution characteristics of the HC intensity and the location of the center of the HC are presented. The Southern Hemisphere HCs in April, May, June, October and November are chosen for further investigation because of the long-term existence of the double-layer structure of these HCs. It can be observed from Table 3 that the upper and lower centers both shift southward to different extents in all the five months. Since the double-layer structure of these HCs is sloped in the vertical direction, we should use the average of the minimum values of the two centers as the intensity of the HC, and we should use the average of the latitude of the two centers as the location of the HC.

We first qualitatively study the evolution characteristics of the HC during the period from 1948—2011, and the quantitative changes of the intensity and location of the center of the HC will be investigated in Section 4.1 and Section 4.2, respectively. Because the

Table 2. Decadal evolution of the double-layer structure of HCs.

	Jan		Feb		Mar		Apr		May		Jun		Jul		Aug		Sep		Oct		Nov		Dec	
	N	S	N	S	N	S	N	S	N	S	N	S	N	S	N	S	N	S	N	S	N	S	N	S
1951—1960	2	0	0	0	0	2	2	**2**	0	**2**	2	**2**	2	0	1	0	0	0	2	**2**	1	**2**	2	2
1961—1970	1	1	0	1	0	1	2	**2**		**2**	2	**1**	1	0	0	0	2	0	1	**2**	1	**2**	2	2
1971—1980	0	2	0	1	0	1	2	**2**	0	**2**	1	**2**	1	0	1	0	2	0	0	**2**	0	**2**	2	2
1981—1990	0	0	0	1	0	2	0	**2**	0	**2**	0	**2**	1	0	1	0	1	0	0	**2**	1	**2**	2	0
1991—2000	0	0	0	0	0	1	0	**1**	0	**2**	1	**2**	2	0	2	0	1	0	0	**1**	0	**2**	1	2
2001—2010	0	0	0	0	0	1	0	**2**	0	**2**	0	**2**	2	0	1	0	1	0	0	**1**	0	**2**	0	0

Table 3. Decadal evolution of the centers (degree latitude) of Southern Hemisphere HCs.

	Apr		May		Jun		Oct		Nov	
	upper	lower	upper	lower	upper	lower	upper	lower	upper	lower
1951—1960	12.5°S	10°S	10°S	7.5°S	7.5°S	7.5°S	7.5°S	7.5°S	10°S	7.5°S
1961—1970	12.5°S	10°S	10°S	7.5°S	7.5°S	7.5°S	7.5°S	7.5°S	10°S	7.5°S
1971—1980	15°S	10°S	10°S	10°S	7.5°S	7.5°S	10°S	7.5°S	10°S	7.5°S
1981—1990	17.5°S	12.5°S	12.5°S	12.5°S	7.5°S	10°S	10°S	7.5°S	15°S	10°S
1991—2000	15°S	12.5°S	12.5°S	10°S	10°S	10°S	10°S	7.5°S	15°S	10°S
2001—2010	15°S	12.5°S	10°S	10°S	10°S	10°S	7.5°S	7.5°S	15°S	10°S

HC is a large-scale overturning circulation with intense convection in the tropics and there exists a double-layer structure in the HC between 850 and 300 hPa, the vertically averaged meridional stream function is used in this section. Fig.4 shows the time evolution (1948—2011) of the zonal mean of the vertically averaged (850–300 hPa) meridional stream function H. It can be observed from Fig.4 that this meridional stream function shows obvious changes in all the five months, suggesting a strong, weak and strong pattern of the strength and poleward shifts of the center and sinking branch of these HCs.

4.1 *Evolution characteristics of the HC intensity*

Referring to Oort and Yienger[32], because there is a double-layer structure in the HC, we use the following definition for the intensity index of the Southern Hemisphere HC (SHCI): For the HC that does not include a double-layer structure, the minimal value of the meridional stream function in the area between 0°–30°S is defined as the SHCI; for the HC that includes a double-layer structure, the average of the two minimal values of the meridional stream function in the area between 0°–30°S is defined as the SHCI. Fig.5 displays the time series (1948—2011) of the monthly mean HC intensity indices in April, May, June, October and November for the Southern Hemisphere. Fig.5 shows that the strength of the Southern Hemisphere HC consistently exhibits decadal variations with a strong, weak and strong pattern in all the five months.

We conduct wavelet transformation analysis on the time series of the monthly mean HC intensity indices, and the real components and wavelet variance are shown in Figs.6 and 7, respectively. It can be observed from Figs. 6 and 7 that there are three major cycles of the SHCI in April, namely, the 12- to 14-year cycle, 25-year cycle and 52-year cycle (the most evident cycle). At the 52-year timescale, the SHCI exhibits decadal variations with a strong, weak and strong pattern, and the points of abrupt change are 1969 and 1996. At the 12- to 14-year timescale, there are four whole cycles of the SHCI. For the SHCI in May, June and October, there are also three major cycles. In May, the three cycles are the 15-year cycle, 27-year cycle and 58-year cycle (the most evident cycle). In June, the three cycles are the 14-year cycle, 22-year cycle and 42-year cycle (the most evident cycle). In October, the three cycles are the 13-year cycle, 22-year cycle and 49-year cycle (the most evident cycle). In November, there are two major cycles, namely, the 24-year cycle and 42-year cycle (the most evident cycle).

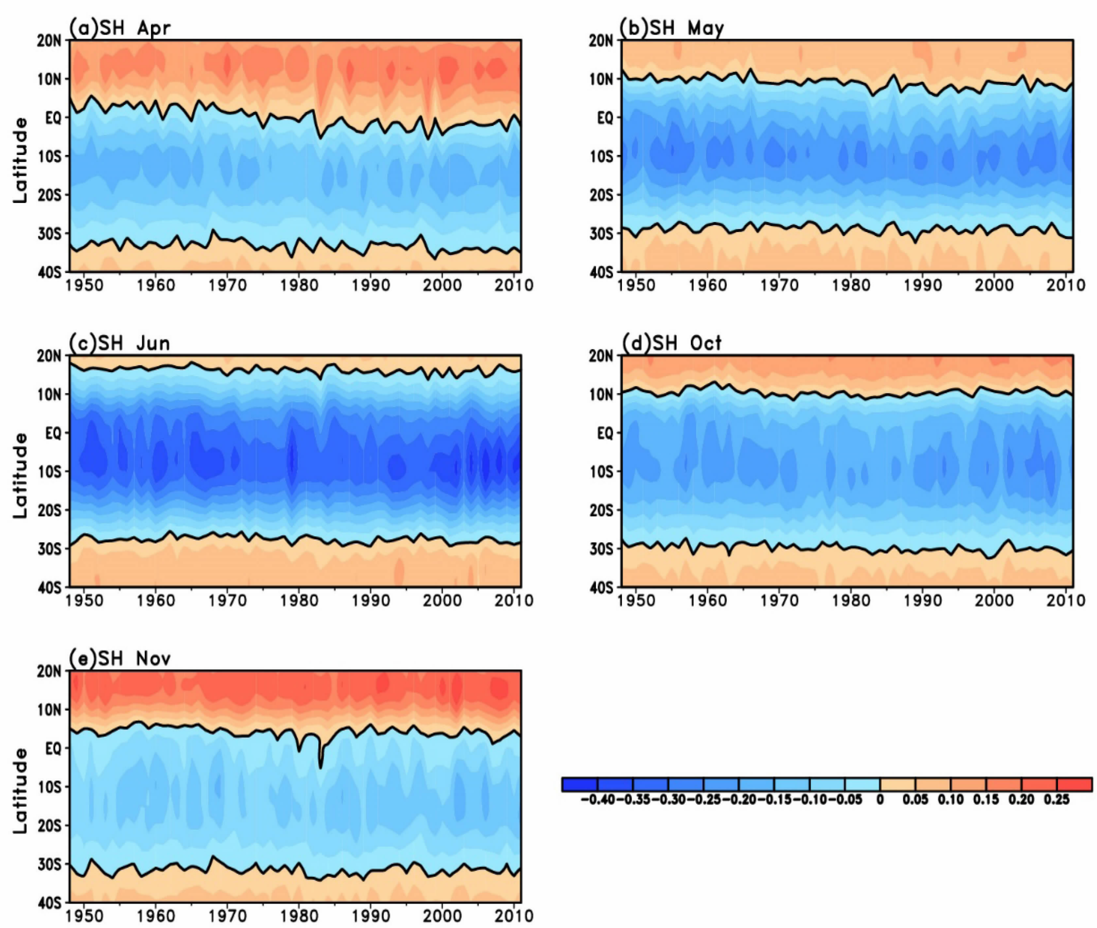

Figure 4. Time evolution (1948–2011) of the zonal mean of the vertically averaged (850–300 hPa) meridional stream function H in (a) April, (b) May, (c) June, (d) October and (e) November for the Southern Hemisphere. The unit of the meridional stream function H is 10^{-6} s^{-1}, and the color interval is 0.05×10^{-6} s^{-1}.

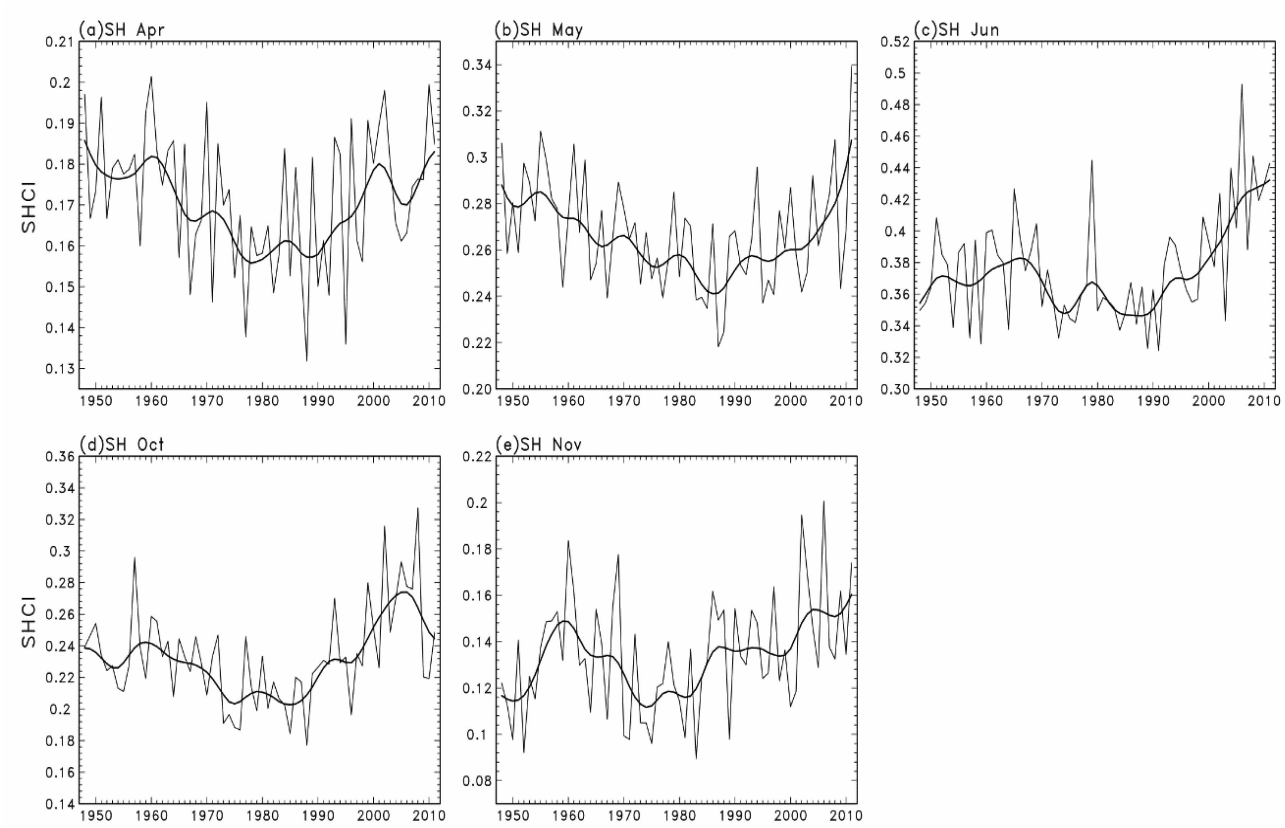

Figure 5. Time series (1948–2011) of the monthly mean HC intensity indices in (a) April, (b) May, (c) June, (d) October and (e) November for the Southern Hemisphere. The bold line in each plot represents the time series with an 11-point Gaussian filter.

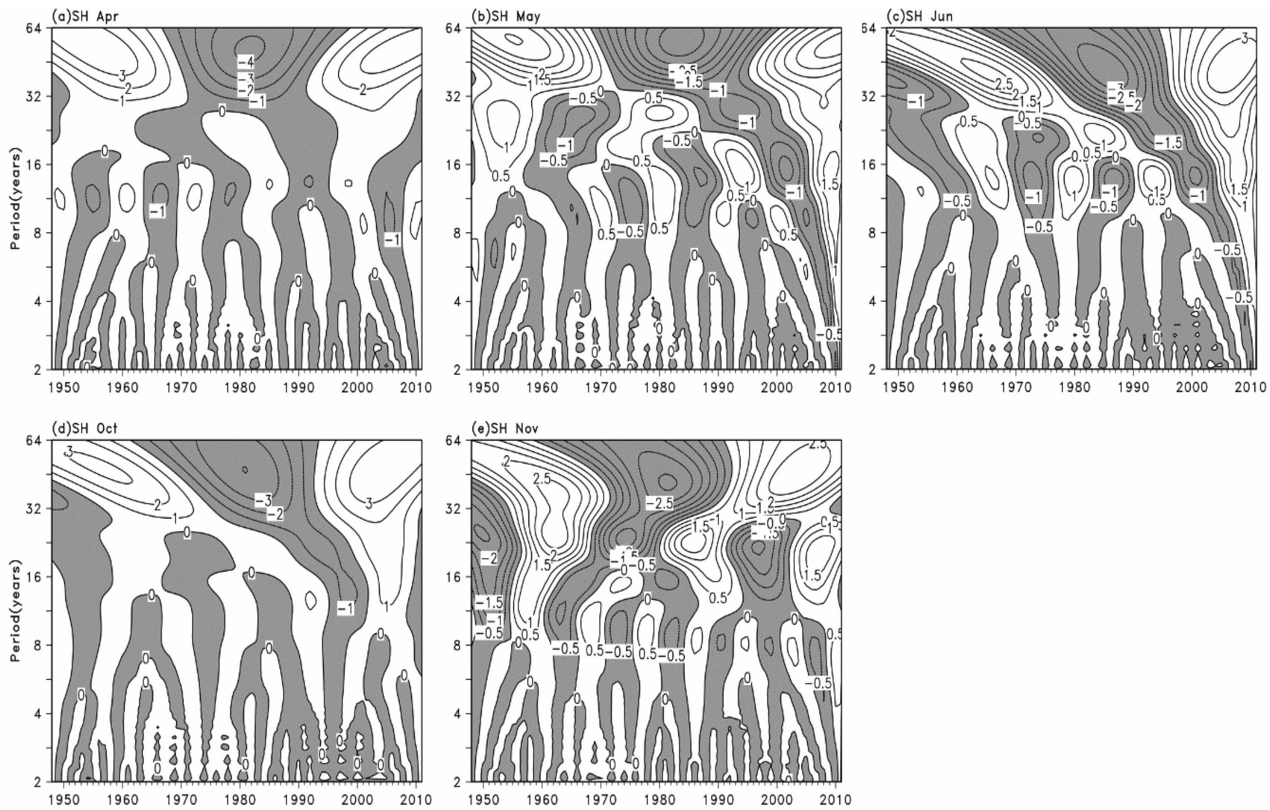

Figure 6. Real components of the wavelet transformation analysis of the HC intensity indices in (a) April, (b) May, (c) June, (d) October and (e) November for the Southern Hemisphere.

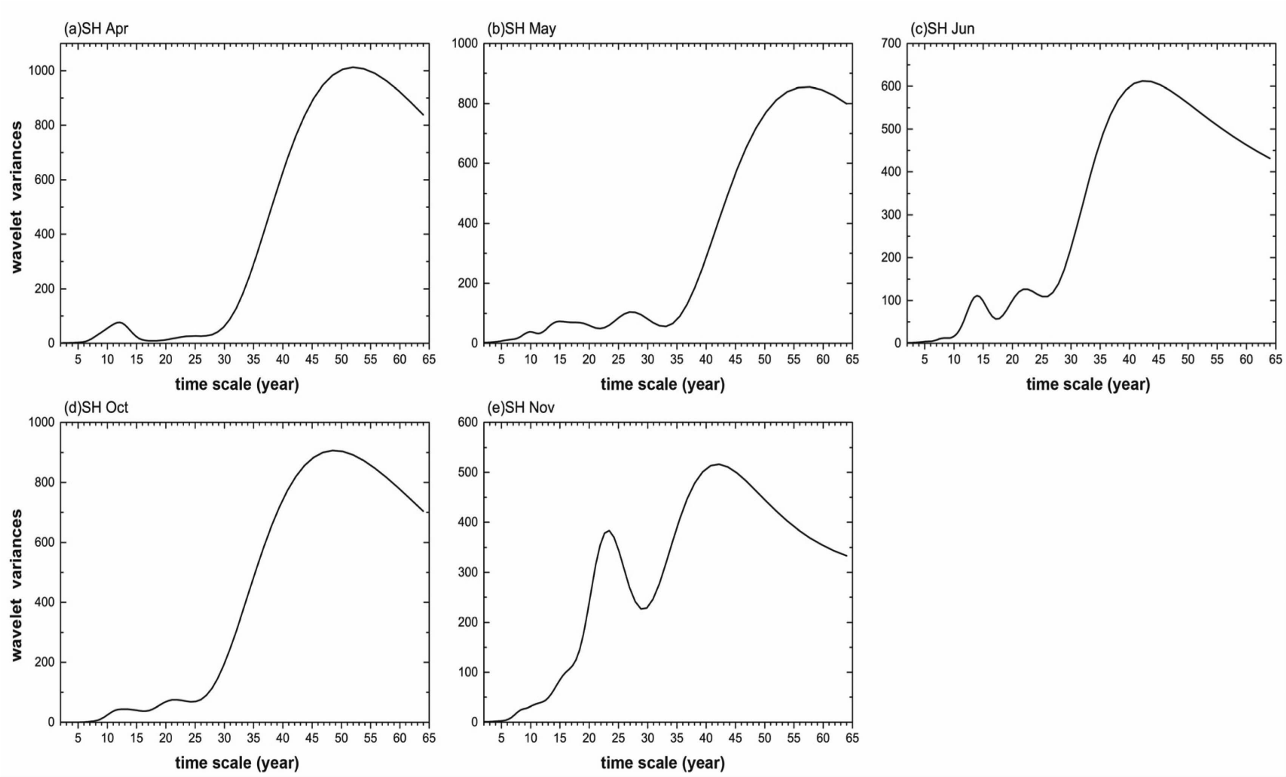

Figure 7. Wavelet variance diagram of the HC intensity indices in (a) April, (b) May, (c) June, (d) October and (e) November for the Southern Hemisphere.

We draw the following conclusions by comparing the wavelet transformation analysis of the HC in the five months. First, there is a 20- to 30-year cycle and a 40- to 60-year cycle of the SHCI in all the five months. Second, except for November, there is a 10- to 15-year cycle of the SHCI. Third, for the 40- to 60-year cycle, the SHCI exhibits a strong, weak and strong pattern in all the five months, namely, the HC intensity is stronger before the 1970s and after the 1990s and weaker during the 1970s and 1990s.

4.2 *Evolution characteristics of the HC center*

Accompanying the changes in the HC intensity, the location of the center of the HC exhibits evident decadal evolution. The double-layer structure of the HC should be considered since this structure is sloped in the vertical direction. For the HC that does not include a double-layer structure, the latitude of the center is defined as the location of the center of the HC; for the HC that includes a double-layer structure, the average of the latitude of the two centers is defined as the location of the center of the HC. The time series of the center of the HC during the period from 1948—2011 are displayed in Fig.8. It can be observed from Fig.8 that the center of the HC in all months except October exhibits a significant (which exceeds the 99% statistical confidence level) poleward shift, with the most prominent poleward shift in April (0.81 degrees per decade) and November (0.9 degrees per decade). The quantitative changes of the center of the HCs in the five months are presented in Fig. 8f, which shows that the center of the HC shifts southward at a rate of 5.18°, 2.11°, 2.50°, 1.79° and 5.76° in April, May, June, October and November, respectively. The mean shift of the center of the HC is 3.47° for the five months.

Given the evident transition of the location of the centers of HCs in the 1980s for all the five months, M-K abrupt change analysis was conducted on the time series of the centers (latitude) of monthly mean HCs. It can be observed from Fig.9 that, except for June, an abrupt transition occurs in 1980 and 1990, namely, the location of the centers of HCs shifts southward after the 1990s, especially in April and November, and this exceeds the 95% statistical confidence level. The location of the center in June shows no evident change. Although there is an intersection of the UF and UB curves, there is no abrupt change in the SHCI in June since the intersection is located at the end of the time period.

According to Figs.8 and 9, the location of the centers of HCs shifts southward after the 1980s, implying poleward shifts of the HCs and thus a poleward shift of the sinking branch of these HCs. The poleward shift of the sinking branch of the HCs may have fundamental impacts on the climate system, including less precipitation and higher frequency of drought in the subtropics (e.g., southwestern Australia, southern Africa), redistribution of rare gases (e.g., ozone), and irreversible changes of the eco-environment, among other effects.

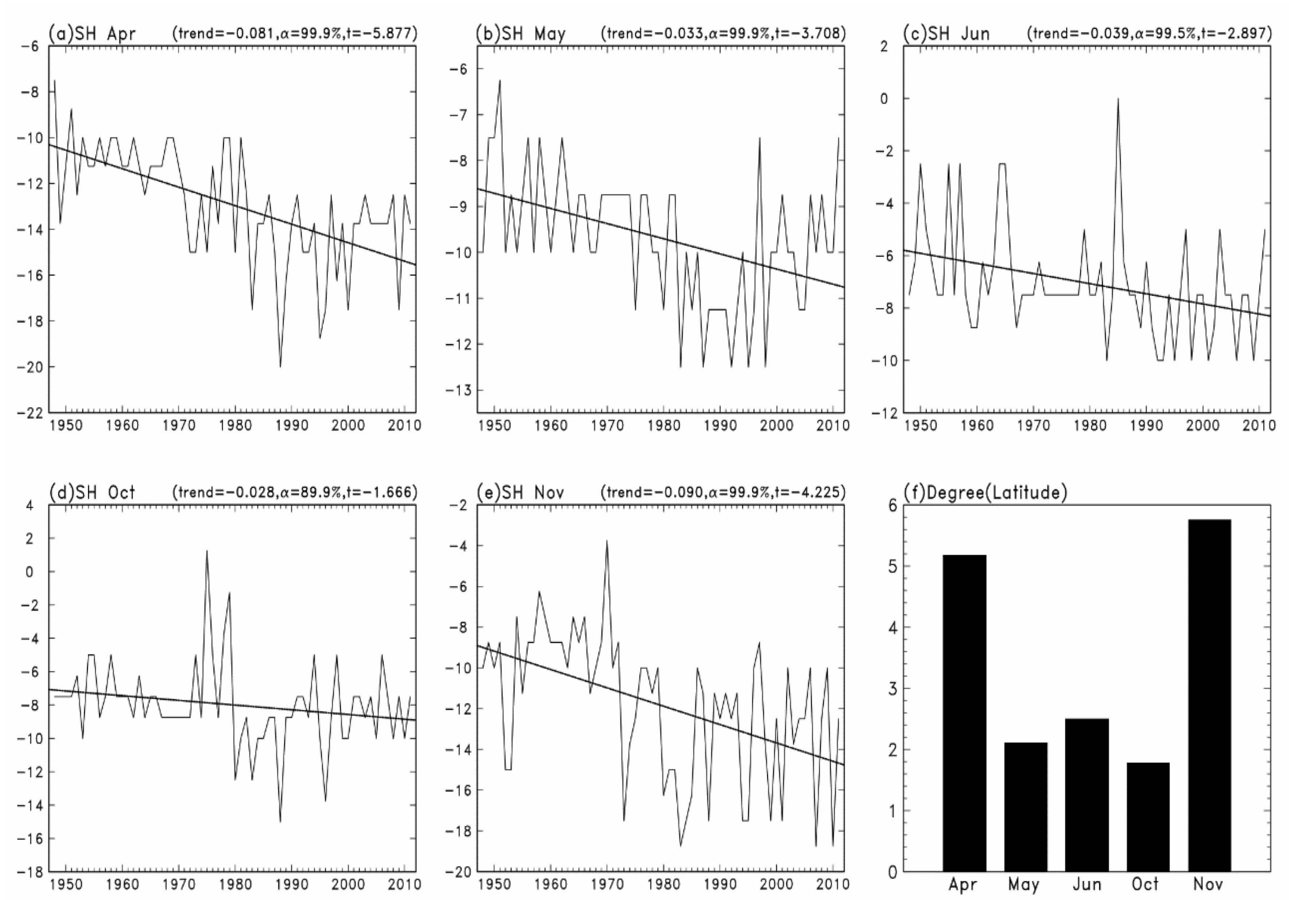

Figure 8. Time series (1948−2011) of the centers (latitude) of monthly mean HCs in (a) April, (b) May, (c) June, (d) October and (e) November for the Southern Hemisphere. The poleward shifts of the centers of the monthly mean HCs are shown in (f). The bold lines in (a)-(e) represent the linear trend of the time series.

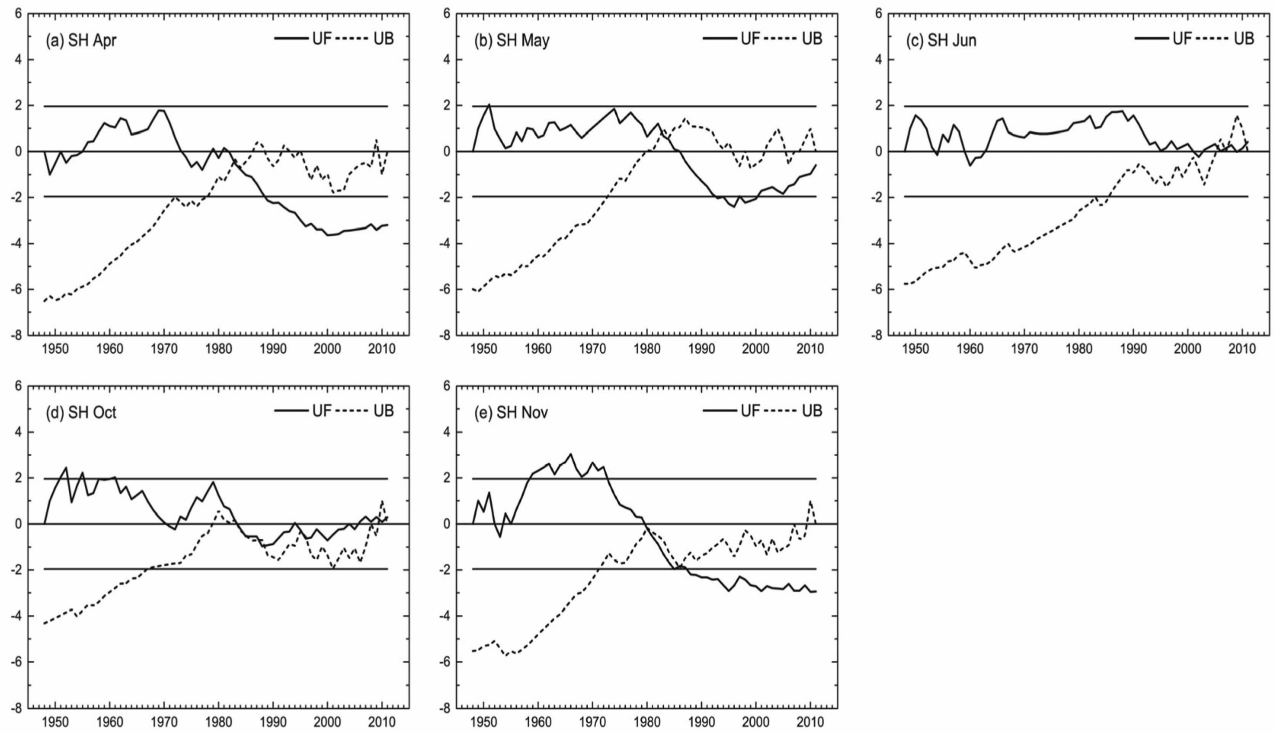

Figure 9. M-K abrupt change analysis of the time series (1948−2011) of the centers (latitude) of monthly mean HCs in (a) April, (b) May, (c) June, (d) October and (e) November for the Southern Hemisphere.

5 CONCLUSIONS AND DISCUSSION

Global atmospheric circulation can be decomposed into 3D horizontal, meridional and zonal circulations using the TPDGAC method. By using the velocity field and stream function of the meridional circulation, we studied the double-layer structure of the HC and its interdecadal evolution characteristics and drew the following major conclusions.

(1) The double-layer structure of the HC is an objective fact, and it constantly exists in April, May, June, October and November in the Southern Hemisphere.

(2) The double-layer structure is more obvious in the Southern than in the Northern Hemisphere. Since the double-layer structure is sloped in the vertical direction, it should be taken into consideration when analyzing the variations of the strength and the center of the HC.

(3) The strength of the double-layer structure of the HC in the Southern Hemisphere consistently exhibits decadal variations with a strong, weak and strong pattern in all the five months (April, May, June, October, November), with a cycle of 20–30 a and 40–60 a.

(4) The centers of the HCs (mean position of the double-layer structure) in the Southern Hemisphere consistently and remarkably shift southward in all the five months. The net poleward shifts over the 64 years are 5.18°, 2.11°, 2.50°, 1.79° and 5.76° for the five respective months, respectively, with a mean shift of 3.47°.

The decadal change of the large-scale HC may lead to a shifting of the climate zones over the globe and higher frequency of extreme weather and climate events, causing considerable social and economic losses. Thus, there has been substantial interest in the evolution characteristics of the intensity and location of the HC. The objective existence of the double-layer structure has been confirmed in this study. Since the double-layer structure is sloped in the vertical direction, the double-layer structure should be taken into consideration when analyzing the changes in the intensity and location of the center of the HC.

The changes in the regional HC cannot be quantitatively studied because the vector method is commonly used. Thus, relative to studies of the zonally averaged HC, there are few studies on the regional HC[33-35]. The stream function and velocity field of the meridional circulation can be determined using the TPDGAC method presented in this study, and the local HC (e.g., the HC in the East Asian monsoon region and the mid-eastern Pacific region) can be investigated. Further investigation concerning the local HC will be undertaken in other studies.

REFERENCES:

[1] WU Guo-xiong, TIBALDI Stefano. Roles of the mean meridional circulation in atmospheric budgets of angular momentum and sensible heat [J]. Chin J Atmos Sci, 1988, 12 (1): 8-17 (in Chinese).

[2] BOWMAN K P, COHEN P J. Interhemispheric exchange by seasonal modulation of the Hadley circulation [J]. J Atmos Sci, 1997, 54 (16): 2045-2059.

[3] WIELICKI B A, WONG T, ALLAN R P, et al. Evidence for large decadal variability in the tropical mean radiative energy budget [J]. Science, 2002, 295 (5556): 841-844.

[4] CHEN J, CARLSON B E, DEL GENIO A D. Evidence for strengthening of the tropical general circulation in the 1990s [J]. Science, 2002, 295 (5556): 838-841.

[5] HU Y, TUNG K K, LIU J. A closer comparison of early and late-winter atmospheric trends in the Northern Hemisphere [J]. J Clim, 2005, 18 (16): 3204-3216.

[6] MITAS C M, CLEMENT A. Has the Hadley cell been strengthening in recent decades [J]. Geophys Res Lett, 2005, 32: L03809, doi:10.1029/2004GL021765.

[7] ZHOU Bou-tao, WANG Hui-jun. Interannual and interdecadal variations of the Hadley Circulation and its connection with tropical sea surface temperature [J]. Chin J Geophys, 2006, 49 (5): 1147-1154.

[8] MA Jie, LI Jian-ping. Strengthening of the boreal winter Hadley circulation and its connection with ENSO [J]. Progr Nat Sci, 2007, 17 (11): 1327-1333.

[9] ZHANG Jun, GU De-jun, SHI Neng. Global mean Hadley circulation intensity index during 1948-2004 and its characteristics [J]. J Nanjing Inst Meteor, 2007, 30 (2): 231-238 (in Chinese).

[10] WU Guo-xiong, TIBALDI Stefano. A scheme for evaluating the mean meridional circulation of the atmosphere [J]. Sci Sinica (Ser B), 1998, 17 (4): 442-450.

[11] WU Guo-xiong, LIU Huan-zhu. Global Time-Averaged Atmospheric Circulation Statistics [M]. Beijing: China Meteorological Press, 1987: 1-20 (in Chinese).

[12] YUE Yang, GUAN Zhao-yong, WANG Pan-xing. Differences of the Bi-level structure of Hadley cells between two different reanalysis data [J]. J Nanjing Inst Meteor, 2005, 28 (5): 695-703 (in Chinese).

[13] QING Yu-Jing, WANG Pan-xing, GUAN Zhao-yong, et al. Comparison of the Hadley cells calculated from two reanalysis data sets [J]. Sci Bull, 2006, 51 (14): 1741-1746.

[14] HU Y, FU Q. Observed poleward expansion of the Hadley circulation since 1979 [J]. Atmos Chem Phys, 2007, 7 (19): 5229-5236.

[15] SEIDEL D J, RANDEL W J. Recent widening of the tropical belt: Evidence from tropopause observations [J]. J Geophys Res, 2007, 112: D20113, doi: 10.1029/2007JD008861.

[16] HUDSON R D, ANDRADE M F, FOLLETTE M B, et al. The total ozone field separated into meteorological regimes-Part II: Northern Hemisphere mid-latitude total ozone trends [J]. Atmos Chem Phys, 2006, 6 (12): 5183-5191.

[17] HU Yong-yun, ZHOU Chen, LIU Ji-ping. Observational

evidence for poleward expansion of the Hadley circulation [J]. Adv Atmos Sci, 2011, 28 (1): 33-44.

[18] FU Q, JOHANSON C M, WALLACE J M, et al. Enhanced mid-latitude tropospheric warming in satellite measurements [J]. Science, 2006, 312 (5777): 1179.

[19] JOHANSON C M, FU Q. Hadley cell widening: Model simulations versus observations [J]. J Clim, 2009, 22 (10): 2713-2725.

[20] HU Yong-yun, TAO Li-jun, LIU Ji-ping. Poleward expansion of the Hadley circulation in CMIP5 simulations [J]. Adv Atmos Sci, 2013, 30 (3): 790-795.

[21] XU Ming. Study on the three dimensional decomposition of large scale circulation and its dynamical feature [D]. Lanzhou University, 2001 (in Chinese).

[22] HU Shu-juan. The three-dimensional expansion of global atmospheric circumfluence and characteristic analyze of atmospheric vertical motion [D]. Lanzhou University, 2006 (in Chinese).

[23] HU Shu-juan. Connection between the short period evolution structure and vertical motion of the subtropical high pressure in July 1998 [J]. J Lanzhou Univ, 2008, 44 (3): 28-32 (in Chinese).

[24] HU Shu-juan, CHOU Ji-fan, CHENG Jian-bo. Three-pattern decomposition of global atmospheric circulation: part I—decomposition model and theorems [J]. Clim Dyn, 2015. doi:10.1007/s00382-015-2818-4.

[25] HU Shu-juan, CHENG Jian-bo, CHOU Ji-fan. Novel three-pattern decomposition of global atmospheric circulation: generalization of traditional twodimensional decomposition [J]. Clim Dyn, 2017, doi: 10.1007/s00382-017-3530-3.

[26] HU Shu-juan, CHENG Jian-bo, XU Ming, et al. Three-pattern decomposition of global atmospheric circulation: part II—dynamical equations of horizontal, meridional and zonal circulations [J]. Clim Dyn, 2017, doi:10.1007/s00382-017-3763-1.

[27] LIU Hai-tao, HU Shu-juan, XU Ming, et al. Three-dimensional decomposition method of global atmospheric circulation [J]. Sci China (Ser D), 2008, 51 (3): 386-402.

[28] DENG Bei-sheng, LIU Hai-tao, CHOU Ji-fan. Analysis of the linkages of large-scale air-sea interaction between the tropical Indian ocean and the Pacific ocean during ENSO events [J]. J Trop Meteor, 2010, 16 (4): 305-312.

[29] GUO Shi-Chang, LI Qiong, LIU Yu, et al. Characteristics of local Hadley circulation and its relation to atmospheric ozone over the low-latitude regions in east Asia [J]. J Trop Meteor, 2012, 28 (4): 478-486 (in Chinese).

[30] QIAN Wei-hong, JIANG Man, SHAN Xiao-long. The physical decomposition principles on atmospheric variables and their application in the analysis of regional rainstorms [J]. Meteor Mon, 2013, 39(5): 537-542 (in Chinese).

[31] KALNAY E, KANAMITSU M, KISTLER R, et al. The NCEP/NCAR 40-year reanalysis project [J]. Bull Amer Meteor Soc, 1996, 77 (3): 437-472.

[32] OORT A H, YIENGER J J. Observed interannual variability in the Hadley circulation and its connection to ENSO [J]. J Clim, 1996, 9 (11): 2751-2767.

[33] QIN Yu-Jing, WANG Pang-xing. Localized Hadley circulation and its linkage to Pacific SSTA [J]. J Trop Meteor, 2011, 17 (4): 352-362.

[34] SHI Neng, FENG Guo-lin, GU Jun-qiang, et al. The climatological variation of global cross-equatorial flow for the period of 1948-2004 [J]. J Trop Meteor, 2007, 13 (2): 201-204.

[35] SEIDEL D J, FU Q, RANDEL W J, et al. Widening of the tropical belt in a changing climate [J]. Nature Geosci, 2008, 1(1): 21-24.

Citation: CHENG Jian-bo, HU Shu-juan and CHOU Ji-fan. The double-layer structure of the Hadley circulation and its interdecadal evolution characteristics [J]. J Trop Meteor, 2018, 24(2): 220-231.